JOURNAL OF COMPUTATIONAL PHYSICS **133,** 113–128 (1997)
ARTICLE NO. CP975658

Complementary Boundary Operators for Wave Propagation Problems

Omar M. Ramahi

Digital Equipment Corporation, PKO3-1/R11, 129 Parker Street, Maynard, Massachusetts 01754
E-mail: ramahi@poboxa.enet.dec.com

Received February 23, 1996; revised September 26, 1996

The complementary operators method (COM) has been shown to be an effective mesh terminator when solving open-region scattering and radiation problems. This study presents the theory of COM and extends it to include general analytical absorbing boundary conditions (ABCs). The COM is applied to the finite difference time domain simulation of electromagnetic problems. The application of COM to elastic and acoustic waves follows in a similar manner. The numerical adaptations of COM to the discretized domain is then discussed to show that careful numerical adaptation is needed to ensure full complementariness of the discretized equations. Numerical experiments will be presented to show the effectiveness of COM in predicting accurate time-domain response as well as critical frequency domain response. In particular, an experiment is detailed that demonstrates how COM can be effective in treating evanescent fields which traditionally have been a major challenge for ABCs in general.

1. INTRODUCTION

The past 10 years have witnessed a dramatic increase in the use of finite methods to solve electromagnetic radiation and scattering problems. In these techniques the space of the problem is mapped in a linear fashion to computer memory; thus, minimizing this space can be of great advantage not only in reducing the memory requirements for the problem, but it also leads to shorter run time. Therefore, imposing the *right* boundary condition becomes, in addition to being a matter of necessity to ensure the complete mathematical description of the problem (well-posedness and uniqueness), a matter of efficiency and practicality. In contrast to the governing PDE equations where one can choose between few well-defined formulations, open region problems offer the user a wide choice of boundary conditions that are not necessarily part of the intrinsic description of the problem.

Boundary conditions have a primary objective: to terminate the computational mesh while maintaining a well-posed, nontrivial, and stable solution. Since the boundary conditions simulate the effect of free space, they are ideally intended to absorb waves impinging upon the boundary from the interior of the computational domain, thus the descriptive name: absorbing boundary conditions (ABCs). These ABCs were originally constructed based on several principles such as the one-way wave equation, asymptotic expansion of the field, or on the pseudo-differential operator theory [1–8]. Aside from the perfectly absorbing boundary condition, which is characterized by nonlocality in space and time, and thus carries with it tremendous cost in implementation, particularly in time-domain techniques [9, 10], most ABCs take the form of a single partial differential equation enforced at artificial boundaries. While the single-equation analytical ABC has shed considerable insight into the mechanism by which waves can be annihilated or partially annihilated at the boundary, these ABCs have stopped short of delivering a level of accuracy that is necessary in many modern and advanced applications. It is important to note here that even if these classical ABCs were enforced at an artificial boundary which is far from the scattering object, high level of accuracy still cannot be guaranteed. In fact, as will be discussed below, the increased space around the structure can increase the error in the solution.

It is perhaps premature at this time to speculate whether the single analytical boundary condition has reached its maximum potential. It is safe, however, to state that the trend in the pursuit of a more effective truncation scheme has deviated from the use of a single analytical expression. The numerical absorbing boundary condition (NABC) and the measured equation of invariance (MEI) [11–13] are techniques in which the ABC is expressed as an algebraic equation whose coefficients are obtained from an auxiliary numerical solution. More recently, another highly effective mesh truncation technique the Berenger's perfectly matched layer (PML) was introduced [14]. The PML medium can be alternatively obtained through a lossy anisotropic mapping [15, 16] and can be described as a scheme of annihilating outgoing waves in a gradual fashion through a series of layers of varying loss. De Moerloose *et al.* [17] have shown that while the PML gives perfect matching for traveling and evanescent waves, in numerical applications,

0021-9991/97 $25.00

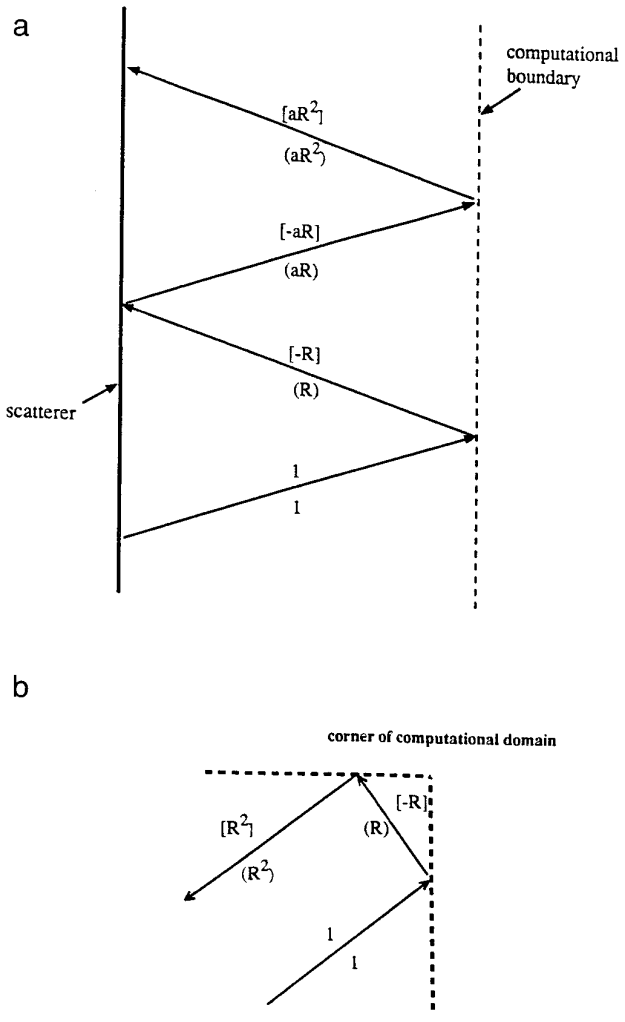

FIG. 1. Illustration of the cancellation of the odd-order reflections: (a) From plane boundaries; (b) from corner regions.

the layer has to be substantially thick to annihilate evanescent waves. Chen *et al.* [18] have shown that through some adjustment of the PML parameters, evanescent waves can be effectively suppressed without affecting the annihilation of the traveling waves. Pekel and Mittra [19] have found that for the PML to provide very high levels of suppression, the boundary layer has to be increased to at least 16, which results in substantial increase in computational cost.

In a recent letter, the complementary operators method (COM) was introduced as a simple, flexible, and parallelizable technique for mesh truncation [20]. In this paper, we present the theory of COM and provide a generalization that extends the method to general (non-Higdon type) single-equation analytical ABCs. We then present the application of COM in the FDTD context and address the significance of numerically correct adaptation of the analytical theory to the discretized domain. Finally, we study the performance of COM with emphasis on its potential for accurate field prediction over wide dynamic range and a wide frequency spectrum.

II. THEORY

Maxwell's equations characterizing the solution of radiation of electromagnetic waves in homogeneous media can be stated as

$$\nabla \times \mathbf{E} = -\mu \frac{\partial \mathbf{H}}{\partial t} \tag{1}$$

$$\nabla \times \mathbf{H} = \varepsilon \frac{\partial \mathbf{E}}{\partial t} + \mathbf{J}, \tag{2}$$

where $\mathbf{E}$ and $\mathbf{H}$ are the electric and magnetic fields in space, and μ and ε are the permeability and permittivity of the medium. The source of excitation is the current $\mathbf{J}$.

When using finite methods to solve for the field in open regions, the infinite domain of the solution has to be truncated to a finite one by artificial boundaries that enclose the source of radiation and the objects that interact with it. On the artificial boundaries, an ABC is enforced to guarantee the well-posedness of the problem. The ABC is not expected to provide complete annihilation of the outgoing waves, and consequently, an error will be introduced in the solution. Since the performance of a particular ABC depends on the location of the mesh-terminating wall, we can arrive at a *measure* of the error caused by the application of the ABC by expressing the total time-harmonic field as a summation of outgoing and incoming waves at the artificial boundary. Suppose we have a computational boundary at $x = a$ and where the interior of the domain is the region on the left-hand side of the boundary. We can express the field at any point to the left of the boundary as

$$U = e^{-jk_x x - jk_y y - jk_z z + j\omega t} + Re^{jk_x x - jk_y y - jk_z z + j\omega t}. \tag{3}$$

Ideally we would like to have zero reflection from the computational boundaries. Therefore, the spurious reflection that is caused by the imperfect absorption of the computational wall is given by the second term in (3)

$$Re^{jk_x x - jk_y y - jk_z z + j\omega t}. \tag{4}$$

Next, we define a complementary ABC as that which if applied to the same problem results in an error of similar magnitude but opposite in phase to what was obtained with the original ABC. Denoting the new solution as U^c, we have

$$U^c = e^{-jk_x x - jk_y y - jk_z z + j\omega t} - Re^{jk_x x - jk_y y - jk_z z + j\omega t}. \tag{5}$$

It follows that the reflections-free solution, or the *numerically exact* solution, denoted as U^{exact} will be the average of the two solutions in (3) and (5):

$$U^{\text{exact}} = \frac{U + U^c}{2}. \tag{6}$$

Unfortunately, in practical applications, this ideal scenario does not take place because of the presence of the radiating structure, the finiteness of the terminating wall and the remaining mesh-terminating boundaries. All these result in multiple spurious reflections of higher orders which do not all cancel when averaging the two solutions as in (6). To demonstrate the mechanism by which these multiple reflections take place, we show in Fig. 1a two vertical lines. The one to the left represents one physical location on the structure, and the one to the right represents one physical location on the boundary. In Fig. 1a, the values in the parenthesis represent incoming and outgoing waves when the ABC is used. The values in brackets represent the solution when the complementary ABC is used. Here, for simplicity, we assume that the structure affects the field by the scaling factor a. Therefore, we clearly observe that when the two solutions are averaged, the odd-order reflections cancel but the even-order reflections do not. In the case of multiple reflections caused by the corners in the computational domain, a similar behavior takes place. Figure 1b shows a corner region. The second reflection of the incident pulse is of an even-order and thus remains unchanged through the averaging of the two solutions. Therefore, regardless of the cause of the even-order and odd-order reflections, the former remain unchanged, whereas the lateral are canceled out.

We make few observations here: first, the cancellation of the odd-order reflections takes place irrespective of the wave number k_x. Therefore, we expect the averaging to be effective even when the fields are traveling and are incident at oblique angles. Second, the averaging of the two solutions also eliminates the odd-order reflections arising even from the structure itself. This effect is expected to be more pronounced in the annihilation of propagating waves than in the evanescent ones. In problems where a significant energy is contained in the evanescent spectrum, the artificial boundary acts as a source which excites a secondary set of evanescent waves that decay in the direction of the scatterer. Therefore, the first reflection of evanescent waves is expected to be the dominant source of error in the evanescent spectrum, and hence, its annihilation can result in significant reduction of spurious errors arising from this part of the spectrum. It is to be emphasized here that this partial annihilation of the reflections due to evanescent energy takes place even if the original ABC (or the complementary ABC) gives total reflection of the evanescent waves.

The discussion above assumed a solution of Maxwell's equations in linear media (where the permeability and permittivity are independent of the fields). For nonlinear media felling the entire computational space, COM is not expected to be effective in general. However, for a nonlinear medium which is finite and localized within the computational space, and, if the field of interest is at locations which are at a distance from the nonlinear medium, COM can be effective. In such case, when the field impinges on one of the terminal boundaries, the localized nonlinear medium plays a role similar to that of the remaining terminal boundaries, thus giving rise to second-order effects which are not annihilated by the COM operation in the first place.

III. COMPLEMENTARY OPERATORS

The simplest complementary pair that can be used is the Dirichlet and Neuman boundary conditions, or the perfect electric conductor and perfect magnetic conductor boundary pair. The use of these boundary conditions as a mean to truncate open-region problems was first introduced by Smith in 1975 [21]. The Dirichlet and Neuman boundary conditions constitute a complementary pair in the sense of the definition given above; however, there implementation can be expensive as demonstrated in the work of Smith. The secondary reflections that arise from either the Neuman or Dirichlet conditions are of the same order as the first-order (primary) reflections (corresponding to $R = 1$ in Fig. 1). Therefore, to obtain reasonably accurate solution, it becomes necessary to push the computational boundaries far away from the scatterer or radiating object so that the secondary reflections are forced out of the solution window. This can be a serious drawback since it counters our primary objective of keeping the boundaries very close to the structure to minimize computer memory. Additional drawback is attributed to reflections from the corners of the computational domain which act in a similar manner to the body of the structure by producing multiple reflections that cannot be filtered out from the correct (reflections-free) signal. This is the case because the second-order reflections taking place at the corners are intermixed with the first-order reflections (because of the very small proximity of the corner region) which are being targeted for annihilation.

The work by Smith can be considered a logical precedent to our presentation here; it cannot be useful in general. For a complementary pair to be effective and efficient in the general treatment of open-region radiation problems, it is necessary to rely upon ABCs which give a reflection coefficient having a magnitude less than one, thus, in essence, simulating the mechanism of damped resonance. Therefore, the potential of realizing high suppression of reflections hinges upon a reasonable performance by the ABC in the first place.

The derivation of ABCs typically begins with some physical principles such as the behavior of the field in the asymptotic region [1], or the assumption that the field in the proximity of the boundary behaves in a predictable fashion, such as in the pseudo-differential equation theory of Engquist and Majda [2]. While the theoretical background may differ, the outcome, in most cases is an analytical expression taking the form of a differential equation (enforced at the artificial boundary). The effectiveness of the ABC is then demonstrated through a quantitative analysis of the reflection coefficient. In this work, the course of development will be the reverse, namely that of synthesizing new ABCs which give rise to a prespecified reflection coefficient.

With our interest in synthesis instead of analysis, we proceed by considering the flexible class of ABCs proposed by Higdon [5, 6]. The generalized form of the N^{th}-order Higdon's ABC is

$$B_N U = \prod_{i=1}^{N} (\partial_x + c^{-1}\xi_i \partial_t + \alpha_i) U = 0, \tag{7}$$

where c is the speed of light, and ξ_i and α_i, $i = 1, 2, 3, \ldots, N$, are constant parameters that can be adjusted to add some degree of flexibility, especially when encountering situations where the field behavior at certain boundaries can be qualitatively predicted. The corresponding reflection coefficient $R[\cdot]$ for time-harmonic fields is found by substituting (3) into (7)

$$R[B_N] = (-1) \prod_{i=1}^{N} \frac{-jk_x + j\xi_i k + \alpha_i}{jk_x + j\xi_i k + \alpha_i}. \tag{8}$$

Higdon's ABC has many attractive features. It has proven to be very versatile and easy to implement. It does not call for any special treatment at the corners, and its independence of tangential derivatives makes it especially useful in treating a wider class of structures [22–25]. Furthermore, Higdon's ABC has been established to be well-posed and stable [6]. However, for Higdon's ABCs of order 3 or higher, the solution can become marginally stable for very low frequency due to computer roundoff [6]. Since many ABCs of the analytical type share similar form (and some are simply equivalent in terms of their reflection properties), computer roundoff problems can be expected whenever higher order ABCs are used [26, 27]. The constants α_i can help stabilize the solution, however, at a cost in performance at very low frequencies.

Aside from the added flexibility that the ξ_i and α_i introduce, these constants can also be manipulated, while leaving purely physical considerations aside, to lead to complementary pairs. By observation, if we set $\xi_N = \alpha_N = 0$ in (8), we arrive at the reflection coefficient

$$R[B_N^c] = (+1) \prod_{i=1}^{N-1} \frac{-jk_x + j\xi_i k + \alpha_i}{jk_x + j\xi_i k + \alpha_i}. \tag{9}$$

The corresponding ABC, denoted by B_N^c is readily found to be

$$B_N^c = \partial_x \prod_{i=1}^{N-1} (\partial_x + c^{-1}\xi_i \partial_t + \alpha_i) U = 0. \tag{10}$$

The new boundary condition in (10) is precisely the complementary version of the ABC in (7) of order $N - 1$. By observation we can express the new ABC as an ∂_x operation on the original ABC of order $N - 1$, viz.,

$$B_N^c = \partial_x B_{N-1}. \tag{11}$$

It is of interest to note here that Higdon has come across the boundary operator $B = \partial_x(\partial_t - c_1\partial_x)$ (see [23, p. 85]) but concluded that it is not optimal in the sense that its reflection properties are equivalent to $B = (\partial_t - c_1\partial_x)$. While the nonoptimality of the complementary operator is clearly evident since the magnitude of the reflection coefficient of both operators is equivalent, the new operator, nevertheless, provides us with the 180° phase shift that we are seeking.

We note here that Higdon's ABC theory has been instrumental in facilitating the synthesis of a complementary pair; however, the treatment can be extended to a wider class of ABCs. This special class includes ABCs which can be expressed by a single analytical differential equation. To demonstrate this, we designate a generic ABC operating at the boundary $x = a$ as β. If ∂_x operates on β, we obtain the new boundary condition β^c:

$$\beta^c = \partial_x \beta. \tag{12}$$

It is a simple exercise to prove that the corresponding reflections coefficient for the time-harmonic field is given by

$$R[\beta^c] = (-1)R[\beta] \tag{13}$$

which demonstrates that β^c is the complementary version of β.

Clearly this generalization is a straightforward procedure; however, caution must be exercised when constructing complementary operators based on other ABCs. It has been shown that Higdon ABCs are well-posed [6], and, therefore, since the complementary operator given in (10) constitute a subset of Higdon ABCs, the well-posedness of the complementary ABC is thusly established. For other analytical ABCs, (12) must be carefully tested to ensure well-posedness.

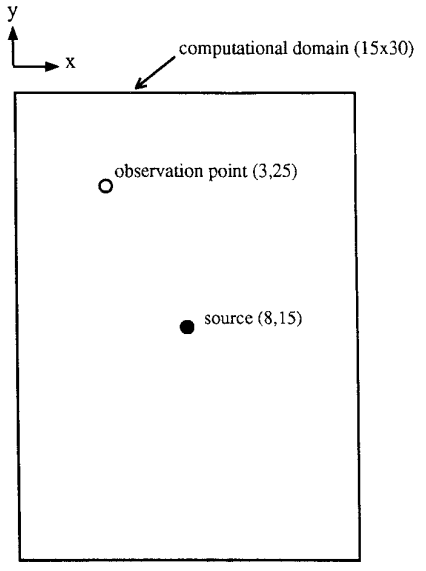

FIG. 2. Geometry for a z-polarized infinitesimal current source radiating in 2D free space (TM polarization).

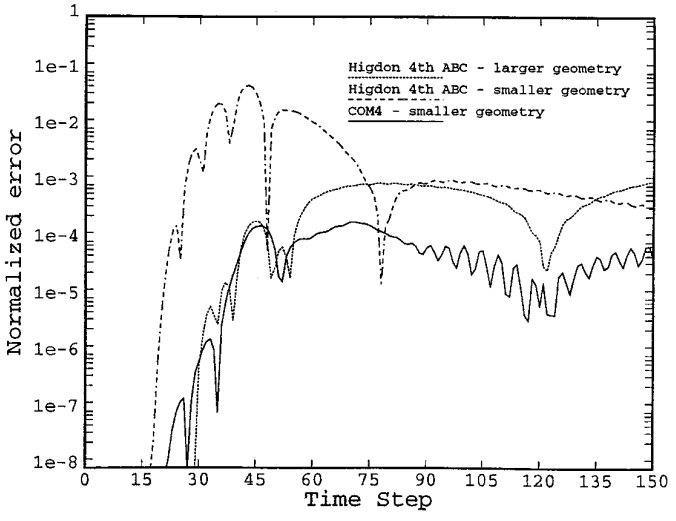

FIG. 3. Normalized error in the total electric field. Smaller domain is of size $15\Delta_x \times 30\Delta_y$ and larger domain is of size $25\Delta_x \times 50\Delta_y$.

IV. APPLICATION IN THE FINITE DIFFERENCE TIME DOMAIN METHOD

The implementation of the ABC calls for transformation from the analytical to the discretized domain. This discretization comes with its own *numerical* errors which should be distinguished from the *theoretical reflection* errors that we typically obtain through (8). These numerical ABC errors can be attributed to several factors that are directly linked to discretization. For instance, consider the reflection coefficient analysis given above (see (8)). When discretizing the wave equation, the wave number k_x is no longer governed by the dispersion relationship in free space, but rather by a more complex equation (see [28, pp. 97–98]). There is no substantial data to indicate whether the numerical errors introduced by the ABC are significant or not. It is highly likely, however, that, irrespective of the differencing scheme adapted, the numerical errors of the FDTD simulation, including the ABC implementation, will put a limit on the overall potentially achievable accuracy. This could be a partial explanation as to why when implementing higher order ABCs; their numerical reflection properties do not necessarily correlate with theory [3, 28].

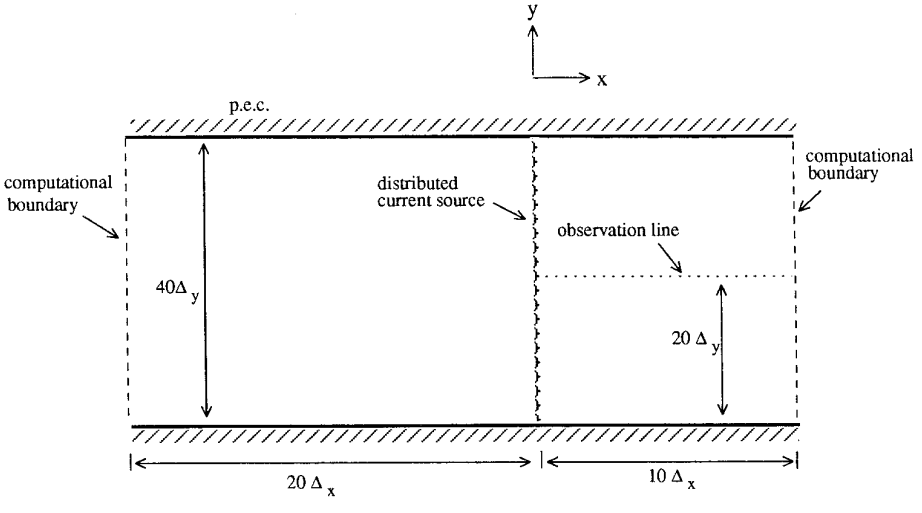

FIG. 4. Geometry for the parallel plate waveguide showing the boundaries specifying the size of the computational domain.

When the theoretical reflection due to the ABC is larger than the discretization errors, it would be fruitless to investigate such discretization errors in great detail. However, the recent development of highly accurate truncation techniques such as Berenger's PML has highlighted the possibility that the discretization errors can put a limit on the accuracy predicted by the theoretical reflection error [29].

In the implementation of complementary operators, the significance of discretization errors become very apparent and very serious to ignore. As we explain below, the discretization of the ABC can lead to a disturbance of the complementariness in the discretized domain unless a correction is made. To see this, we express the solution to the finite-difference scheme as

$$U_\Delta(n_x, n_y, n_z, n_t) = e^{-jk_x n_x\Delta_x - jk_y n_y\Delta_y - jk_z n_z\Delta_z + j\omega n_t\Delta_t} + \mathrm{Re}^{jk_x n_x\Delta_x - jk_y n_y\Delta_y - jk_z n_z\Delta_z + j\omega n_t\Delta t}. \quad (14)$$

The field, U_Δ, is defined at discrete points in space, $x = n_x\Delta_x$, $y = n_y\Delta_y$, and $z = n_z\Delta_z$, and the discrete points in time, $t = n_t\Delta_t$; Δ_x, Δ_y, and Δ_z are the mesh spacing in x, y, and z, and Δ_t is the time step. Using a differencing scheme that was found to be accurate and stable [2, 22], the boundary condition (7) takes the form

$$B_{N,\Delta}U = \prod_{i=1}^{N} [I + a_i S^{-1} + b_i T^{-1} + c_i S^{-1}T^{-1}]\, U_\Delta(n_x, n_y, n_z, n_t) = 0, \quad (15)$$

where

$$a_i = \frac{-1 + \xi_i\Delta_x/c\Delta_t + \alpha_i\Delta_x/2}{1 + \xi_i\Delta_x/c\Delta_t + \alpha_i\Delta_x/2}$$

$$b_i = \frac{1 - \xi_i\Delta_x/c\Delta_t + \alpha_i\Delta_x/2}{1 + \xi_i\Delta_x/c\Delta_t + \alpha_i\Delta_x/2}$$

$$c_i = \frac{-1 - \xi_i\Delta_x/c\Delta_t + \alpha_i\Delta_x/2}{1 + \xi_i\Delta_x/c\Delta_t + \alpha_i\Delta_x/2},$$

and I, S, and T, are the identity, space shift, and time shift operators, respectively, defined by

$$IU_\Delta(n_x, n_y, n_z, n_t) = U_\Delta(n_x, n_y, n_z, n_t)$$
$$SU_\Delta(n_x, n_y, n_z, n_t) = U_\Delta(n_x + 1, n_y, n_z, n_t)$$
$$TU_\Delta(n_x, n_y, n_z, n_t) = U_\Delta(n_x, n_y, n_z, n_t + 1).$$

Substituting (14) in (15) we obtain the time-harmonic reflection coefficient of the discretized operator,

$$R[B_{N,\Delta}] = \prod_{i=1}^{N} \frac{1 + a_i e^{jk_x\Delta_x} + b_i e^{-j\omega\Delta_t} + c_i e^{jk_x\Delta_x - j\omega\Delta_t}}{1 + a_i e^{-jk_x\Delta_x} + b_i e^{-j\omega\Delta_t} + c_i e^{jk_x\Delta_x - j\omega\Delta_t}} e^{-2jk_x n_x\Delta_x}, \quad (16)$$

where n_x corresponds to the location of the terminal boundary.

Following the same procedure, we can derive the reflection coefficient that corresponds to the discretized operator in (10). When $\xi_N = \alpha_N = 0$, the discretized boundary operator coefficients for $i = N$ reduce to $\alpha_i = -1$, $b_i = 1$, $c_i = -1$. We have

$$R[B^c_{N,\Delta}] = \frac{1 - e^{jk_x\Delta_x} + e^{-j\omega\Delta_t} - e^{jk_x\Delta_x - j\omega\Delta_t}}{1 - e^{-jk_x\Delta_x} + e^{-j\omega\Delta_t} - e^{-jk_x\Delta_x - j\omega\Delta_t}} R[B_{N-1,\Delta}]. \quad (17)$$

This expression can be simplified to

$$R[B^c_{N,\Delta}] = (-1)\, e^{jk_x\Delta_x} R[B_{N-1,\Delta}]. \quad (18)$$

Phase terms appearing in the expression for reflection coefficients have traditionally been ignored since they do not contribute to the magnitude of the reflection coefficient. For the COM operators, as can be seen from the above analysis, this is not the case. The phase term $e^{jk_x\Delta_x}$ can have a pronounced effect on the complementariness of the operators.

This phase term depends on the propagation number and the node spacing in the direction normal to the boundary. We notice that for $e^{jk_x\Delta_x}$ to equal 1, thus ensuring full complementariness, one or more of the following conditions should hold: the Δ_x spacing shrinks to zero, the frequency goes to zero, or the traveling wave impinges on the boundary at very oblique angles. Unfortunately, all these scenarios are very impractical. To alleviate this numerical nuisance, we again exploit the flexibility inherent in Higdon's ABC that permitted the construction of the complementary ABC in the first place. To this end, we set $\alpha_N = 0$ and $\xi_N = A$ in (7), where A is a constant, whose purpose will be clear shortly, to arrive at a new ABC,

$$B^{c*}_N = (\partial_x + c^{-1}A\partial_t) \prod_{i=1}^{N-1} (\partial_x + c^{-1}\xi_i\partial_t + \alpha_i)U = 0 \quad (19)$$

with the corresponding reflection coefficient:

$$R[B^{c*}_N] = \frac{-jk_x + jAk}{jk_x + jAk} \prod_{i=1}^{N-1} \frac{-jk_x + j\xi_i k + \alpha_i}{jk_x + j\xi_i k + \alpha_i}. \quad (20)$$

If we take the limit as $A \to \infty$ we have

$$\lim_{A\to\infty}(R[B^{c*}_N]) = \prod_{i=1}^{N-1} \frac{-jk_x + j\xi_i k + \alpha_i}{jk_x + j\xi_i k + \alpha_i}. \quad (21)$$

In the limit as $A \to \infty$, B^{c*}_N becomes equivalent to the original ABC in (7). However, the functionality of B^{c*}_N

becomes evident when we express the reflection coefficient in the discretized domain,

$$\lim_{A\to\infty}(R[B^{c*}_{N,\Delta}]) = \frac{1 + e^{jk_x\Delta_x} - e^{-j\omega\Delta_t} - e^{jk_x\Delta_x - j\omega\Delta_t}}{1 + e^{-jk_x\Delta_x} - e^{-j\omega\Delta_t} - e^{-jk_x\Delta_x - j\omega\Delta_t}} R[B_{N-1,\Delta}], \tag{22}$$

simplifying to

$$R[B^{c*}_{N,\Delta}] = e^{jk_x\Delta_x} R[B_{N-1,\Delta}]. \tag{23}$$

The extra phase term in (23) is equivalent to that in (18) and thus full complementariness is now achieved in the discretized domain. The constant A does not pose any numerical hazard, as can be seen when inserted in the expression for the boundary operator B_Δ, yielding $a_N = 1$, $b_N = -1$, and $c_N = -1$. Numerical experiments have shown that the results are insensitive to A as long as $A > 1000$.

Finally, we note[1] that an equivalent operator to $\lim_{A\to\infty}(B^{c*}_N)$ can also be obtained by the operator $\partial_t B_{N-1}$. It is a simple exercise to show that both of these operators give reflection coefficients that are identical in both the analytic and discretized domains.

In summary, the two operators that are complementary in both the analytical and the discretized domains are

$$\partial_x \prod_{i=1}^{N-1} (\partial_x + c^{-1}\xi_i\partial_t + \alpha_i)U = 0 \tag{24}$$

and

$$\partial_t \prod_{i=1}^{N-1} (\partial_x + c^{-1}\xi_i\partial_t + \alpha_i)U = 0. \tag{25}$$

The discussion presented here, namely the balancing of the effect of the complementary operators in the discretized domain, can be extended in a straightforward manner to develop complementary operators for linear non-Higdon type ABCs.

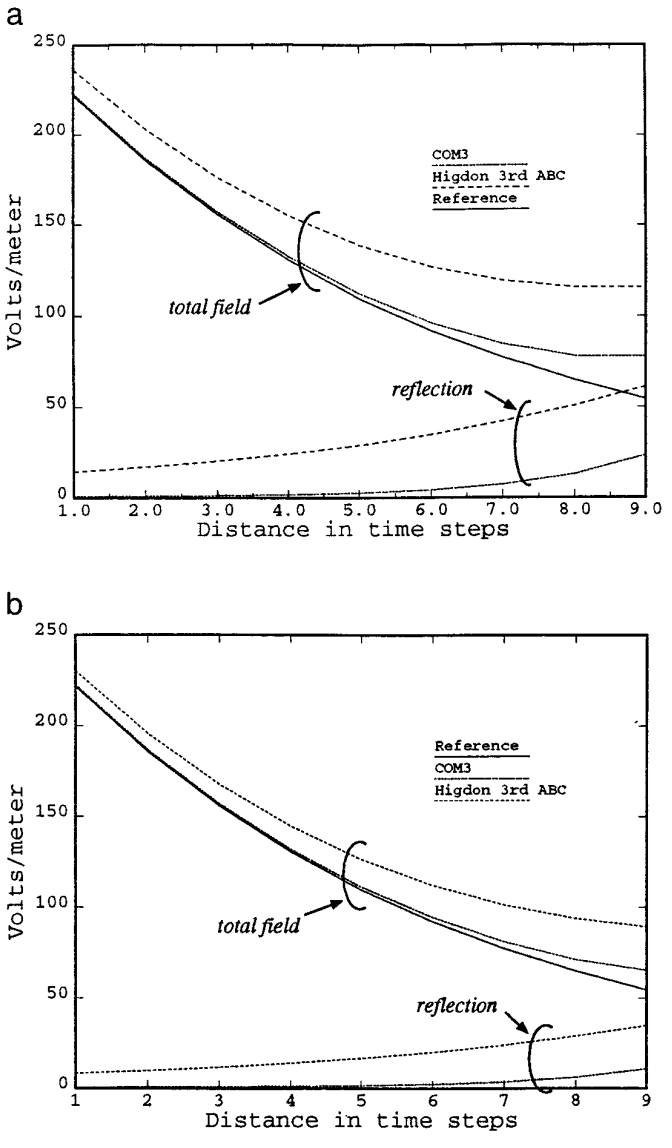

FIG. 5. Electric field along the axis of the parallel plate waveguide for $\lambda = 25\Delta_x$: (a) $\alpha_i = 0$; (b) $\alpha_i = 0.05$.

V. NUMERICAL EXPERIMENTS

Previous research [3] has shown that a quantitative evaluation of ABCs or mesh truncation techniques in general can be difficult. In [3] harmonic analysis in cylindrical coordinates was used to show that the ABC's performance strongly depends on the harmonic content of the radiating (scattered) field which depends on the shape of the scattering body and its size. Furthermore, in 2D as well as 3D space, finite geometries such as a cynlinders, spheres, or boxes, there is no fine transition between the evanescent and traveling modes. In fact there are no purely traveling or purely evanescent waves either [3]. This makes a quantitative evaluation of ABCs very difficult indeed. Another important consideration is that the reflection properties that are typically discussed in conjunction with ABCs (such as in this work) are based on the highly convenient steady-state time-harmonic analysis which does not take into account transients, or more precisely, pure time-domain effects. This very important point was recently highlighted by Kamel [30] who showed, through the simple example of radiation from a dipole radiator, that the time-domain reflection coefficient should not necessarily mirror that

[1] See Acknowledgment at end of paper.

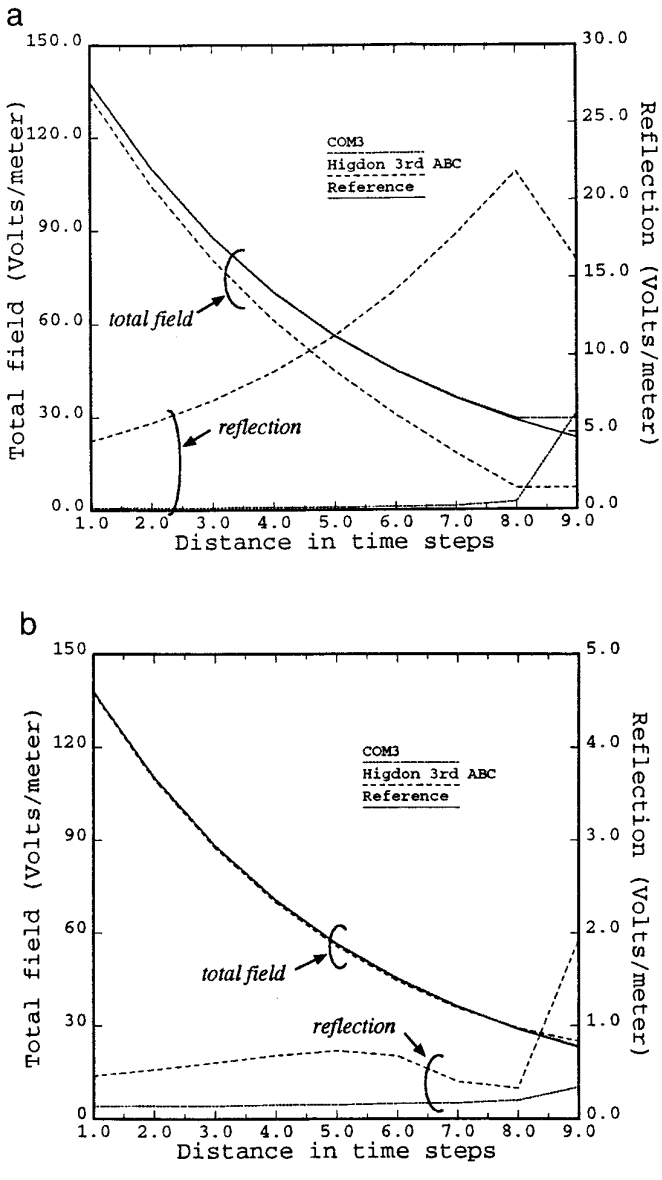

FIG. 6. Electric field along the axis of the parallel plate waveguide for $\lambda = 30\Delta_x$: (a) $\alpha_i = 0$; (b) $\alpha_i = 0.05$.

obtained from the time-harmonic assumptions. The study in [30] could explain, in part, why when higher order ABCs are tested (as in [28, Chap. 7]), the accuracy obtained does not correlate to the expected performance of either the analytical or numerical expressions.

Another important consideration when evaluating ABCs is that the performance of a certain ABC cannot be expected to be uniform over the entire computational domain. As was shown in Fig. 1(a), the effect of artificial reflections that arise from evanescent waves is strong when the observation point is chosen close to the boundary and these reflections diminishes as the structure is approached. Therefore, testing an ABC for its absorption of evanescent waves require careful selection of observation points.

Despite the difficulty in developing quantitative methodology for the analysis of ABCs, qualitative studies can be highly important in revealing the relative strength of one truncation technique over another. In this work, we consider several examples in 2D and 3D space. Solutions obtained using COM are denoted, as COM*N*, where *N* would indicate the order of the operators used. For all the examples presented, comparison is made with Higdon's ABCs and the reference solution which is obtained by solving the problem in a computational domain large enough to force out any artificial reflections from the boundaries while enforcing a fourth-order Higdon ABC.

A. *Infinitesimal Source Radiating in 2D Space*

In the first test, we solve the problem of radiation in 2D space. The source of radiation is an idealized current source (point source in 2D space) that is invariant in the z-direction. Figure 2 shows the current source centered in a $15\Delta_x \times 30\Delta_y$ computational space, where $\Delta x = \Delta_y = \Delta_s = 15$ mm. The time step is $\Delta_t = 31.84$ ps, chosen slightly below the Courant limit to ensure the stability of the FDTD time marching scheme. For this problem, we use an excitation function that gives a very smooth time transition:

$$f(t) = \begin{cases} 15\omega_1 \sin(\omega_1 t) - 6\omega_2 \sin(\omega_2 t) + \omega_3 \sin(\omega_3 t), & 0 \le t \le t_0, \\ 0, & \text{otherwise}, \end{cases}$$

where $t_0 = 10^{-9}$ and $\omega_i = 2\pi i/t_o$, $i = 1, 2, 3$.

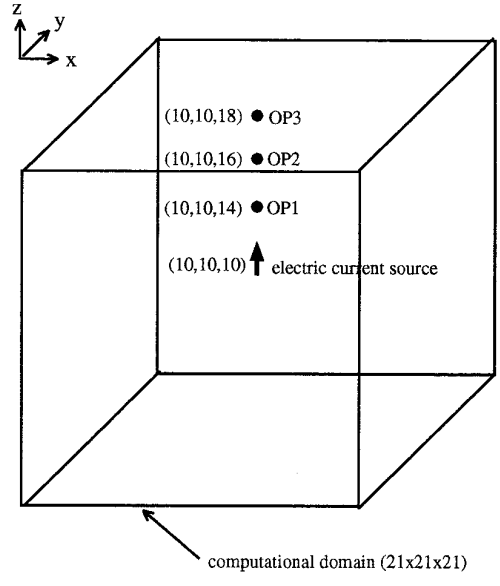

FIG. 7. Geometry for a *z*-oriented Hertzian dipole in 3D space.

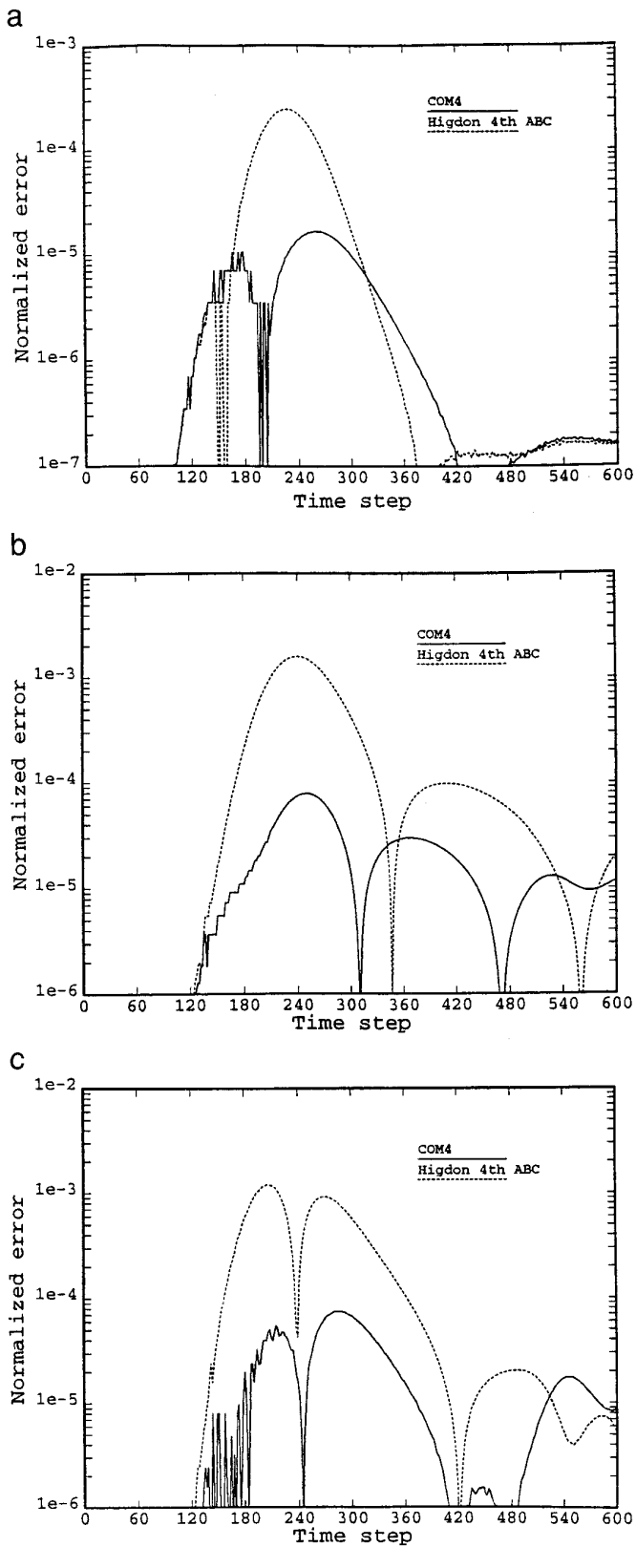

FIG. 8. Normalized error at OP1: (a) in E_x; (b) in E_z; (c) in H_x.

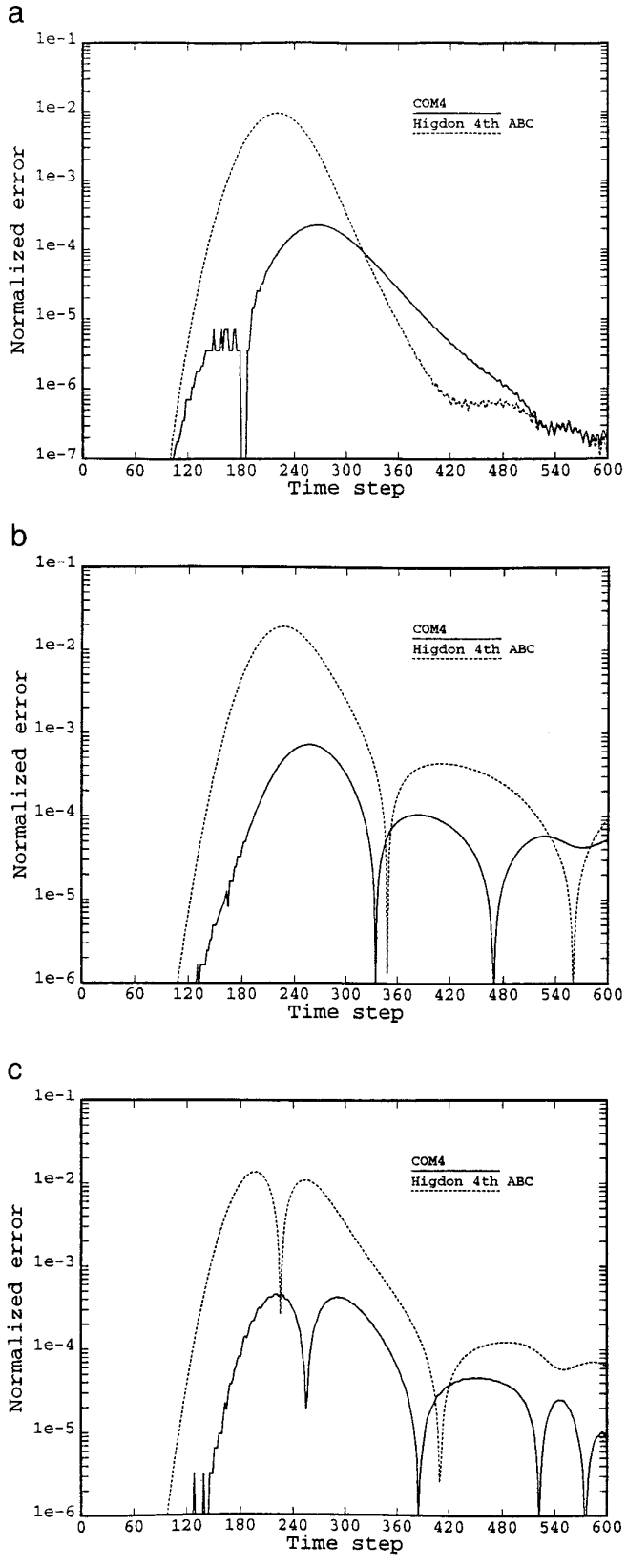

FIG. 9. Normalized error at OP2: (a) in E_x; (b) in E_z; (c) in H_x.

The field is evaluated at the observation point (OP) located at $(3\Delta_s, 25\Delta_s)$. The field at this particular location contains near field low frequency evanescent fields as well as high frequency traveling waves with oblique incidence. Figure 3 shows the normalized error, $E_{\text{error}}^{\text{norm}}(t)$, which is defined according to the following formula:

$$E_{\text{error}}^{\text{norm}}(t) = \frac{E_{\text{abc}}(t) - E_{\text{ref}}(t)}{\max|E_{\text{ref}}(t)|}, \tag{26}$$

where $E_{\text{abc}}(t)$ is the solution obtained in the small geometry using COM or Higdon's ABC, and $E_{\text{ref}}(t)$ is the reference solution.

Also shown in Fig. 3, the field as the same observation point, but computed with a computational domain of size $25\Delta_x \times 50\Delta_y$. Even though the larger computational domain is approximately double the size of the one used earlier, Higdon fourth-order ABC did not give the accuracy obtained by *COM*4 in the smaller domain. In fact, we notice that the maximum error calculated using Higdon fourth-order ABC in the larger domain is approximately one order of magnitude larger than that obtained using *COM*4 in the smaller domain. However, if it is considered that the accuracy obtained using Higdon fourth-order ABC in the larger domain is satisfactory, solving the problem twice, as would be needed in *COM*4 implementation, would still be more efficient than running the larger domain problem with Higdon's fourth-order ABC. In the case of the smaller geometry with COM4 implementation, the memory requirement and the number of operations needed are c_1N and $2c_2N$, respectively, where N is number of cells in the smaller computational domain and c_1 and c_2 are constants that depend only on the FDTD implementation. In the case of larger geometry with Higdon fourth-order ABC implementation, the memory requirement, and the number of operations needed are approximately $2c_1N$ and $2c_2N$, respectively. Since computer memory is a more scarce and expensive resource than time, the effectiveness of COM4 can easily be realized.

B. *Response of COM to Purely Evanescent Waves*

In this test we study the effectiveness of COM in reducing artificial reflections arising from evanescent fields by constructing an experiment in which the radiated field can be carefully controlled to consist of only evanescent energy. To this end, we consider the problem of a parallel plate waveguide which extends infinitely along its axis as shown in Fig. 4. This waveguide is considered to be elementary in the study of waveguiding structures; however, it can offer unique insight into the interaction of evanescent fields with ABCs.

For a z-invariant radiating source (TM polarization), the field can be resolved into numerable modes (discrete

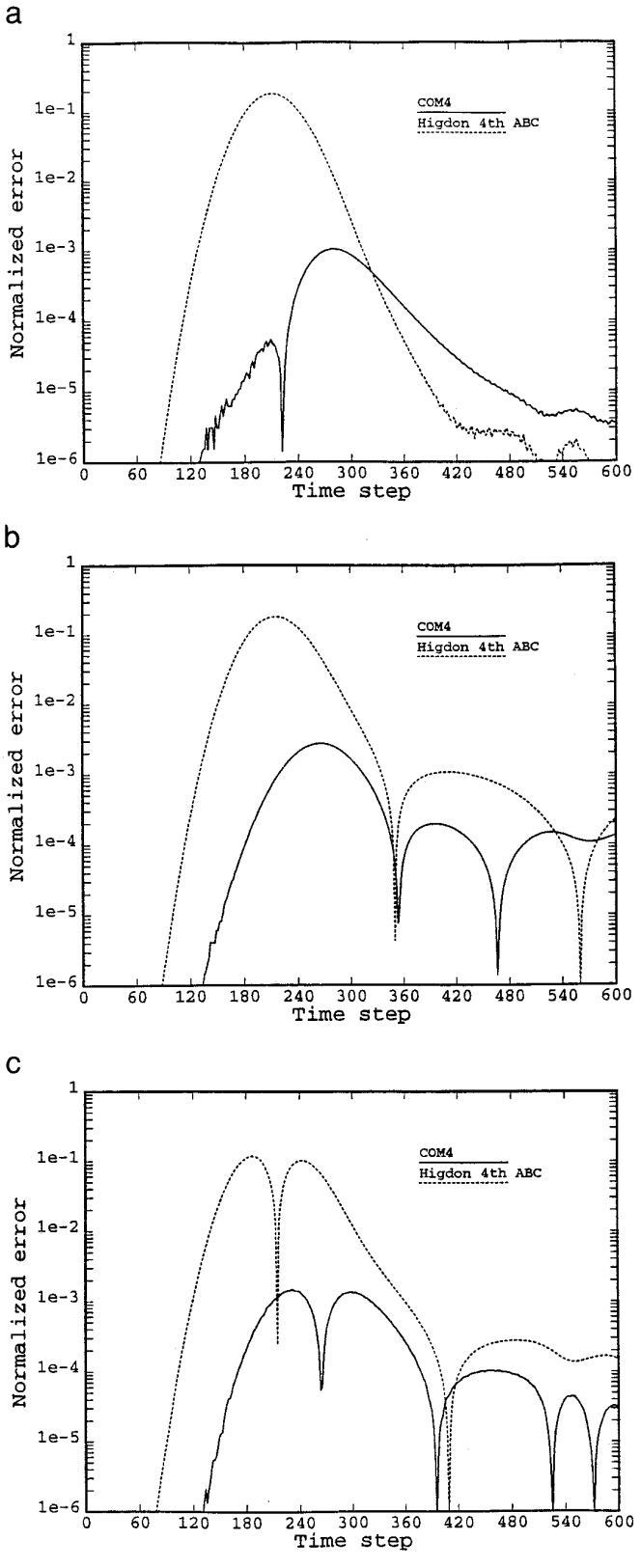

FIG. 10. Normalized error at OP3: (a) in E_x; (b) in E_z; (c) in H_x.

spectra). The excitation of each mode depends on the source frequency. For a frequency below the cutoff frequency, f_c, the field will be evanescent. To generate a single evanescent mode, we use a current source which is typically used for excitation of waveguide modes. This source is a sheet of current positioned along a plane transverse to the axis of the guide as shown in Fig. 4. The excitation of the current sheet and its distribution (vector quantity) is given by

$$\mathbf{K}(x,y) = \hat{\mathbf{z}} \cos\left(\frac{2\pi}{W} y\right) \delta(x)(1.0 - e^{-0.01^9 t}) \sin\left(ct \frac{2\pi}{\lambda}\right); \quad (27)$$

$\delta(.)$ is the Derac-delta function, c is the speed of light, and W is the width of the waveguide. Because the source is turned on at a fixed time during the simulation, the smoothing multiplier, given by $(1.0 - e^{-0.01^9 t})$ is introduced to minimize the effects of unwanted transients that can lead to both traveling and evanescent modes. For this current source, the analytical solution in the region right of the source is given by

$$E_z(x,y) = \cos\left(\frac{\pi}{a} y\right) e^{-jx\sqrt{(\omega/c)^2 - (\pi/W)^2}}. \quad (28)$$

When the excitation frequency is less than $f_c = \pi/W$, the value under the radical is imaginary, thus giving a single evanescent mode with a unique decay constant.

Let $\Delta_x = 15$ mm, $\Delta_y = 3.75$ mm, and $W = 150$ mm. The computational domain is limited to the area shown in Fig. 4. Our objective here is to study the isolated response of the ABC at the right-hand terminal boundary, and for this we chose the left-hand terminal boundary to be at a farther distance from the source such that the reflections caused by it are negligible. Next, we generate two separate modes for two different frequencies below f_c. Although the analytical solution for this problem is available, we shall not make any comparison with this solution since it does not include the discretization effects and other FDTD artifacts which need to be preserved to isolate the effect of the ABC or COM.

The FDTD simulation is run for 50,000 time steps to guarantee the dissipation of any transients (which might include traveling waves.) The magnitude of the field of the resulting time-harmonic response is extracted by sampling the peak of the wave over the last 1000 time steps of the simulation.

As explained earlier, COM is expected to annihilate the first-order reflection of evanescent waves. The constants α_i that were originally introduced by Higdon to help in stability can also help in the absorption of evanescent waves since k_x is imaginary and the magnitude of the reflection coefficient will be less than unity. For each of the

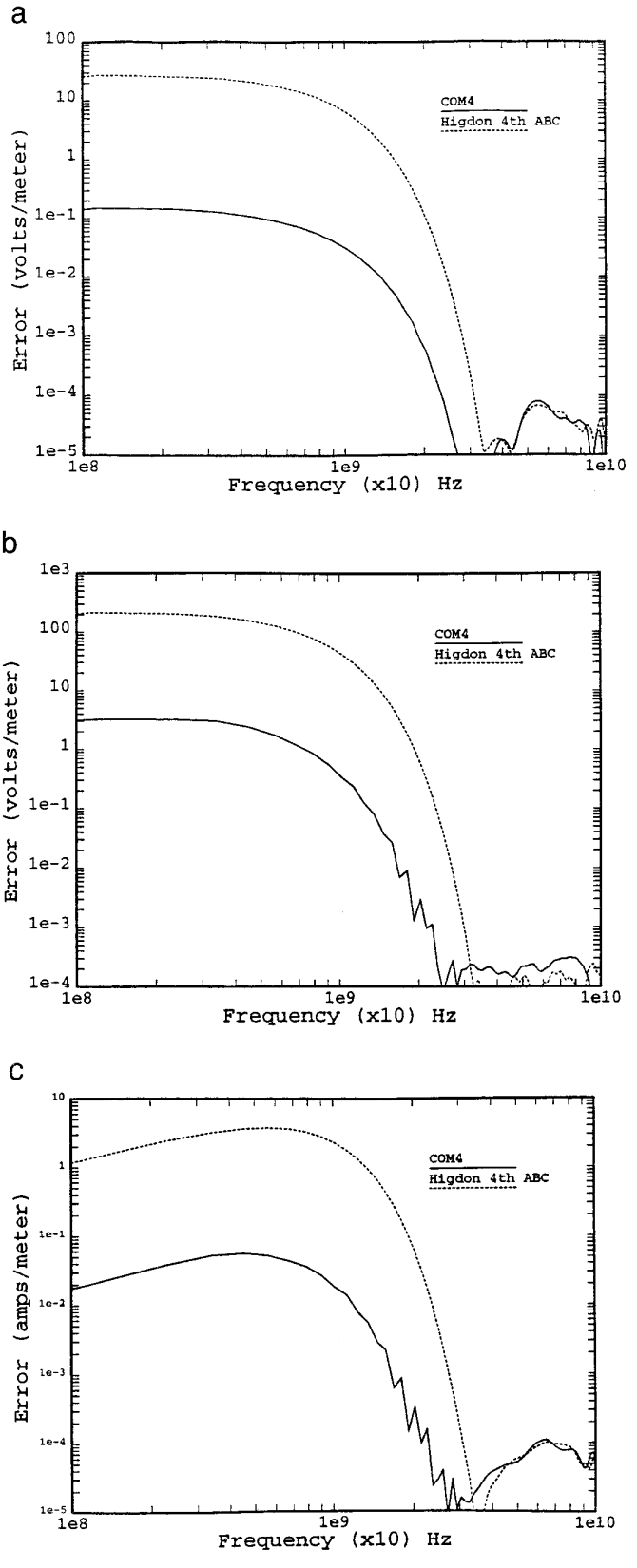

FIG. 11. Frequency spectrum of the error signal at OP3: (a) in E_x; (b) in E_z; (c) in H_x.

two modes studied, we present results for two different tests: $\alpha_i = 0$ and $\alpha_i = 0.05$.

We consider two time-harmonic excitations below cutoff: $\lambda = 25\Delta_x$ and $\lambda = 30\Delta_x$. Figures 5 and 6 show the total and reflected fields. The reflected field, E_{error} is calculated by $E_{\text{error}}(t) = E_{\text{abc}}(t) - E_{\text{ref}}(t)$. From these results, we see that COM can lead to a significant reduction in the error from evanescent waves even if no loss factor, α_i, is introduced. Furthermore, we clearly observe that the reflected waves that arise from the enforcement of ABCs at the boundary are decaying exponentials. This gives validity to the interpretation of the ABC as a source of evanescent waves that decay in the direction of the source. Which leads to the conclusion that the effect of the ABC on the reflected evanescent waves is more pronounced as the observation point approaches the computational boundary.

C. *Hertzian Dipole Radiating in 3D Space*

For the third example, we turn to the problem of radiation in 3D space. We first discuss a representative problem where a Hertzian dipole of length Δ_z is placed in free space. The geometry is detailed in Fig. 7. The artificial boundary is placed 10 cells from the source. The dimensions are $\Delta_x = \Delta_y = \Delta_z = \Delta_s = 1$ mm. The excitation function of the source is given by

$$f(t) = -2(t - t_o)e^{(-(t-t_o)/(2T_w))^2}, \tag{29}$$

where t_o is a time offset and T_w is the width of the pulse set to $20\Delta_t$.

The size of the computational domain is $21\Delta_s \times 21\Delta_s \times 21\Delta_s$. Three observation points chosen are: OP1 at $(10\Delta_s, 10\Delta_s, 14\Delta_s)$; OP2 at $(10\Delta_s, 10\Delta_s, 16\Delta_s)$; and OP3 at $(10\Delta_s, 10\Delta_s, 18\Delta_s)$. The time-domain response is shown in Figs. 8–10 for the normalized error in the electric and magnetic fields of different polarizations. (For these particular observation points, $E_x = E_y$, $|H_x| = |H_y|$, and $H_z = 0$.) Here, we used a very small loss factor $\alpha_i = 0.008$ such that stability is maintained while not adversely affecting the low frequency response.

We make several observations here: The reduction of the error due to COM4 is more appreciable as the observation point approaches the boundary. This supports the earlier assertion that COM suppresses evanescent waves effectively. Also, as the distance to the boundary increases, the reduction in the error as provided by COM remains appreciable compared to Higdon's fourth-order ABC; however, it is important to note that the error level due to Higdon's fourth-order ABC is already low at these locations that further improvement seems superfluous.

Let us look at OP3 in more detail. The calculated results for the fields at this observation point show a sizable reduction of the error over the time range where the pulse has most of its energy. To obtain a measure of the performance with respect to frequency, or to determine how the COM affects the different frequencies that constitute the input signal, we use the discrete Fourier transformation (DFT) to obtain the frequency spectrum of the calculated pulse. Figure 11 shows the frequency spectrum of the error signal for the fields at OP3. *COM*4 is shown to give approximately two orders of magnitude improvement over Higdon's fourth-order ABC. Note that in Fig. 11, the input pulse has very little energy beyond 30GHz which makes the response of ABCs beyond this frequency inconclusive.

D. *Hertzian Dipole Radiating in the Presence of a Perfectly Conducting Plate*

In this experiment we study the problem of wave–object interaction. Here our objective will be to study the perfor-

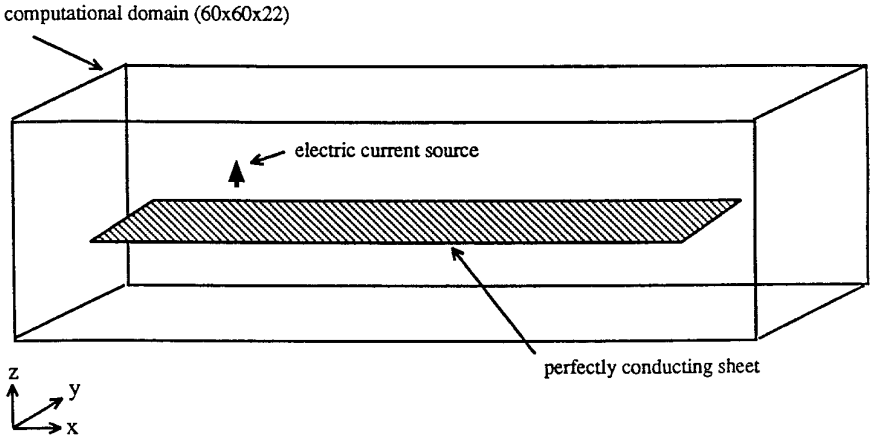

FIG. 12. Geometry for a z-oriented Hertzian dipole adjacent to a perfectly conducting sheet.

mance of COM when predicting the field due to an electric current source radiating in close proximity to a perfectly conducting plate. The geometry for this problem is shown in Fig. 12. For this practical example, we bypass the time domain results and present the calculated fields as a function of the frequency spectrum using DFT.

We chose a moderate size square plate of 40mm × 40mm. The cell dimensions are $\Delta_x = \Delta_y = \Delta_z = \Delta_s =$ 1 mm. The artificial boundary is placed 10 cells from the nearest source or plate edge giving a computational domain of $60\Delta_x \times 60\Delta_y \times 22\Delta_z$. The source of radiation is a z-oriented Hertzian dipole of length Δ_z with a time excitation function given in (29). The current source is positioned two cells above the plate at $(30\Delta_x, 20\Delta_y, 12\Delta_z)$. The reference solution was obtained for a larger geometry where the terminal boundary was positioned 110 cells from the nearest source or plate body giving a computational domain of $260\Delta_x \times 260\Delta_y \times 222\Delta_z$.

Two observation points are chosen: OP1 selected at $(30\Delta_x, 20\Delta_y, 20\Delta_z)$ such that it is close to the source thus being in the near field while at the same time being very close to the boundary to study the behavior of evanescent waves. The second, OP2, is chosen at $(20\Delta_x, 40\Delta_y, 20\Delta_z)$ in order to study the response of COM to obliquely incident waves.

In this experiment, which has a more practical flavor than the cases considered before, we express the results in terms of the source-normalized fields which is defined as

$$\tilde{E}_{\text{norm}}(f) = \frac{|\tilde{E}(f)|}{|\tilde{J}(f)|}, \tag{30}$$

where $\tilde{E}$ and $\tilde{J}$ are the Fourier transforms of the electric field and the current source, respectively.

Expressing the radiated fields in this fashion gives a uniform frequency response which takes into account the variation of the magnitude of the frequency harmonics comprising the output signal.

In Fig. 13, we show the normalized fields for E_x, E_y, and E_z for OP1. These results show that the field obtained using *COM*4 can hardly be distinguished from the reference solution while Higdon's fourth ABC gives an error which grows to a maximum of approximately 8 dB towards the lower frequencies. Figure 14 gives the frequency spectrum of the normalized error (normalized error in time domain was first obtained according to (26) and the Fourier transformed). *COM*4 is seen to give a dramatic reduction in the error which explains the high accuracy observed in the final field calculation.

Similar calculations are presented for OP2 in Figs. 15 and 16. Here we see that as in OP1, *COM*4 give a solution which is within a fraction of a decibel from the reference solution. By looking at the error spectrum, the improvement over Higdon's fourth ABC is observed to be more

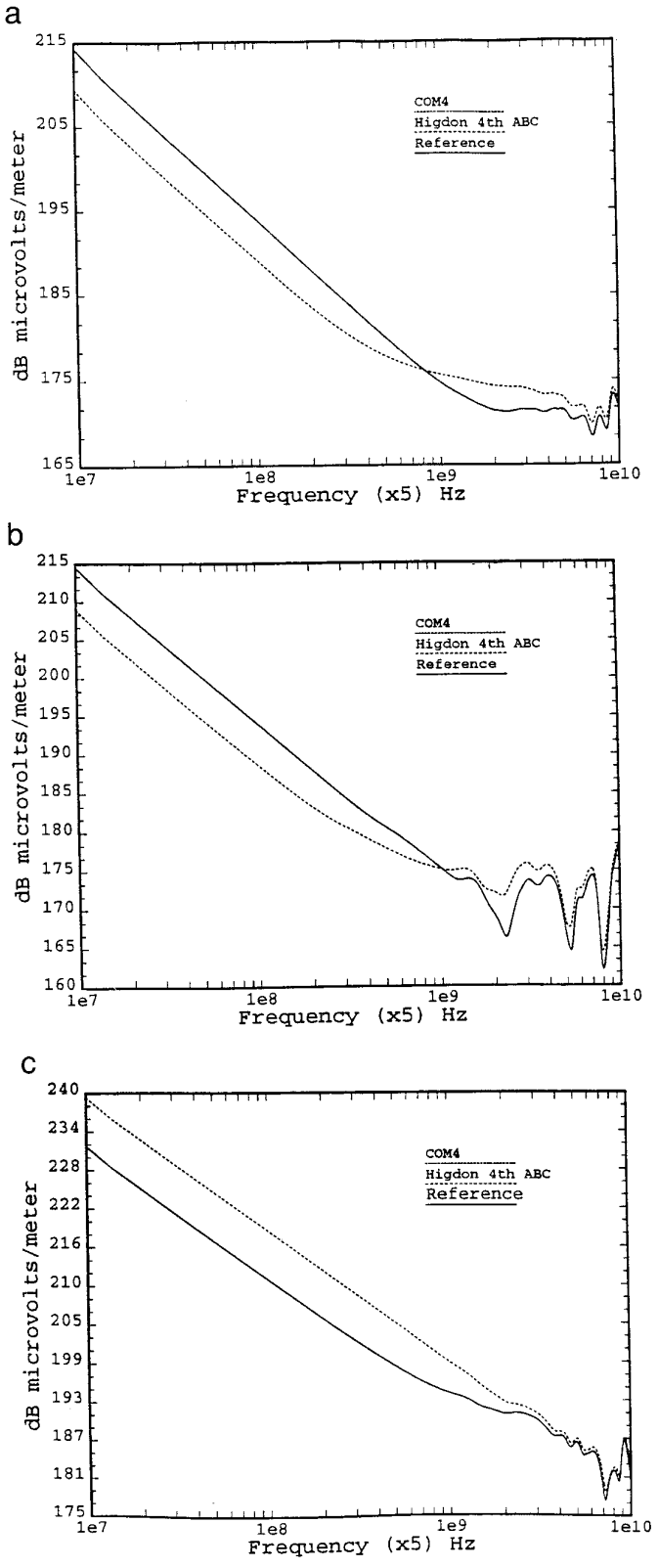

FIG. 13. The source-normalized field at OP1 for the plate problem: (a) E_x; (b) E_y; (c) E_z.

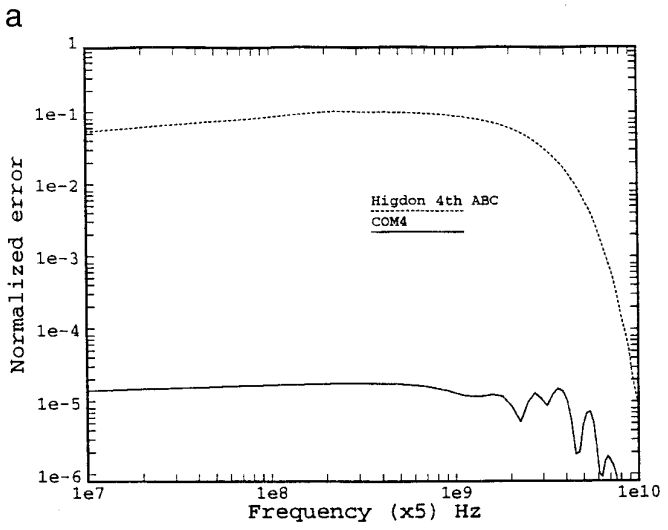

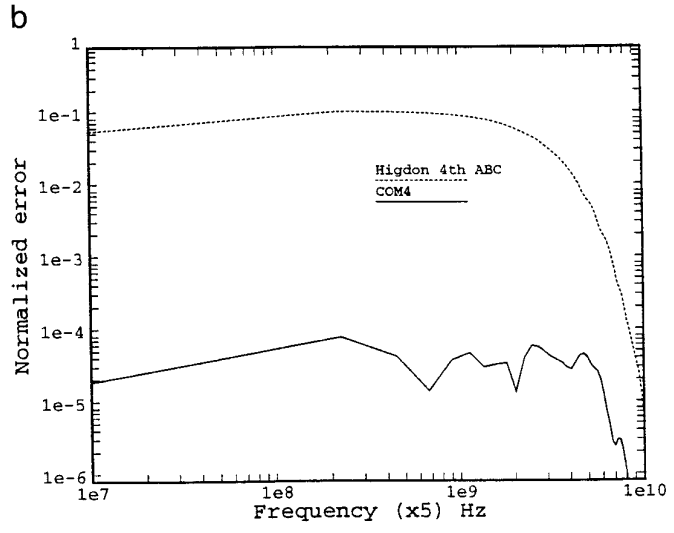

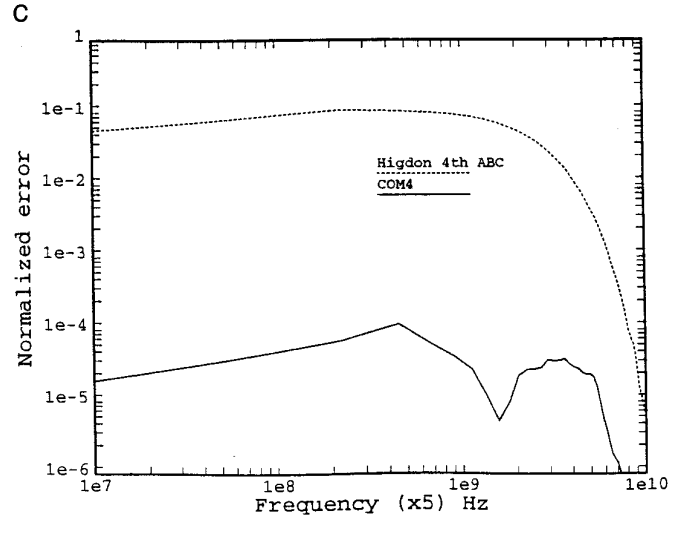

FIG. 14. Frequency response of the normalized error at OP1 for the plate problem: (a) in E_x; (b) in E_y; (c) in E_z.

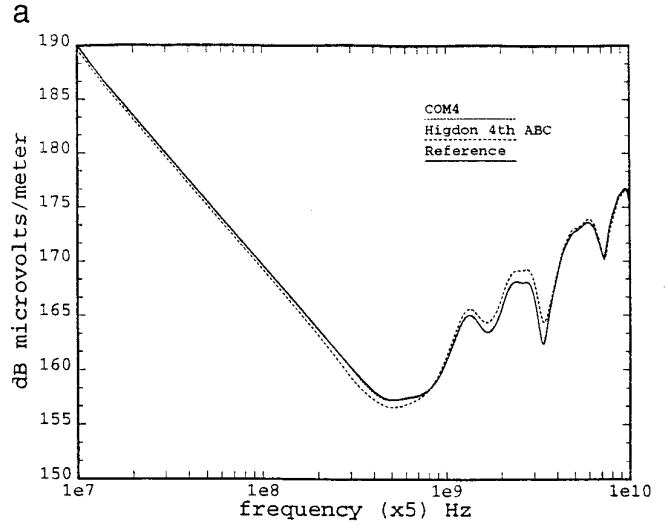

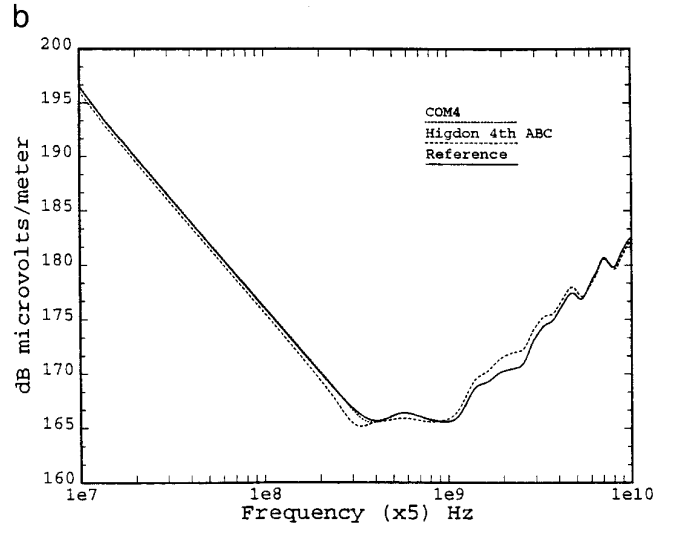

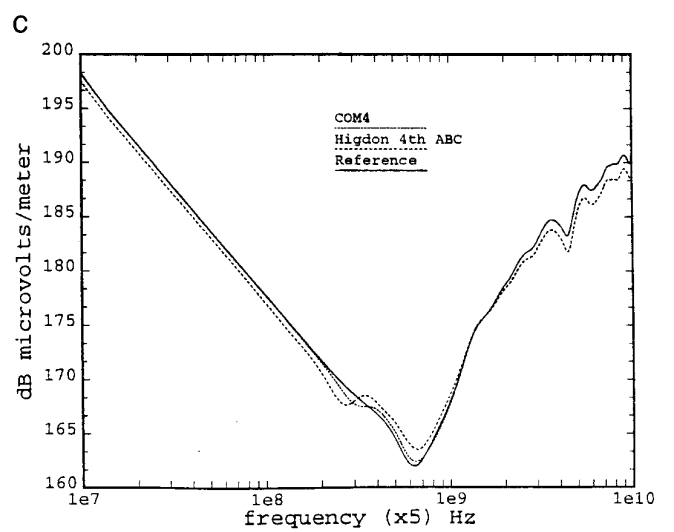

FIG. 15. The source-normalized field at OP2 for the plate problem: (a) E_x; (b) E_y; (c) E_z.

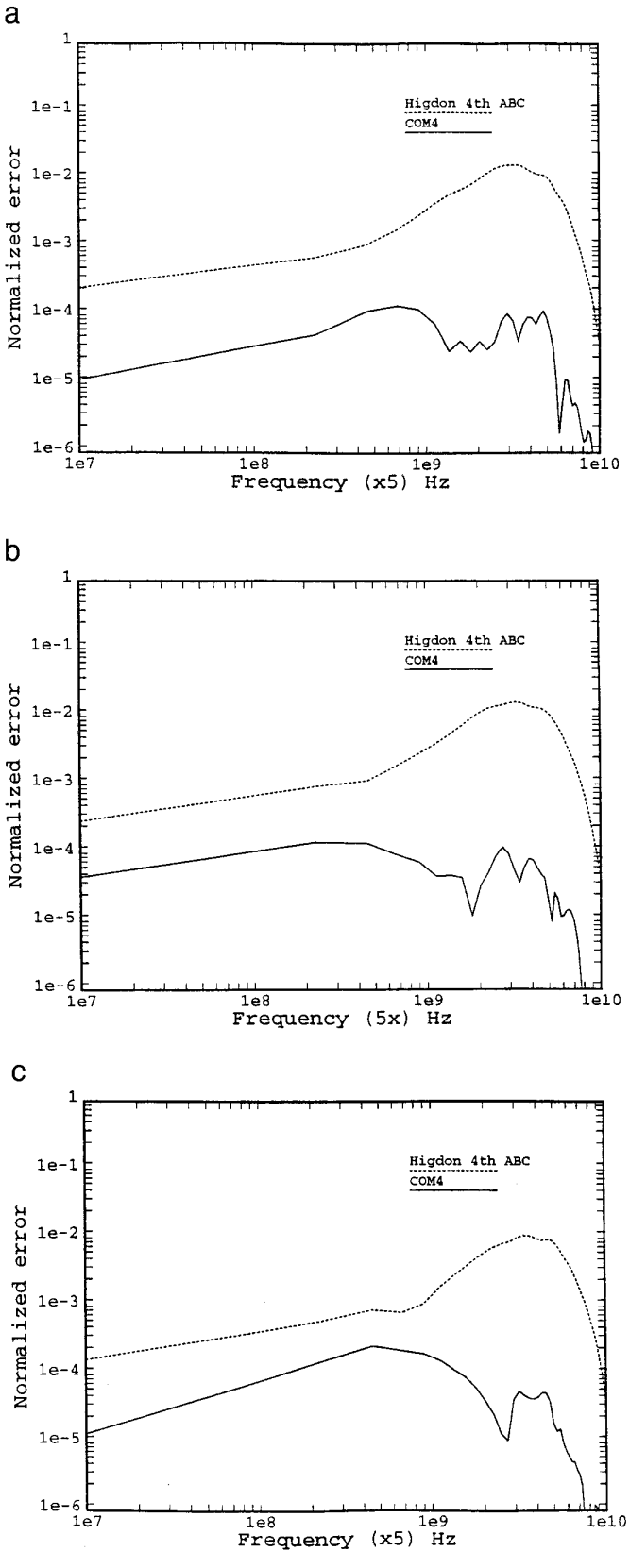

FIG. 16. Frequency response of the normalized error in at OP2 for the plate problem: (a) in E_x; (b) in E_y; (c) in E_z.

pronounced over the higher frequencies since the Higdon's ABC is more sensitive to oblique incident waves which can be dominant at this observation point.

VI. CONCLUSION

In this work, we presented the theory of complementary operators as a method for truncating the computational domain when solving open region radiation problems. The development was based on Higdon's ABC operators since they are naturally suited for synthesis of the new unconventional operators that comprise the complementary pair. The extension to non-Higdon type ABCs was then directly deduced. While the emphasis in this work was on the solution of Maxwell's equations, the applicability extends in a uniform fashion to the solution of acoustic and elastic waves in open media.

Numerical examples were presented which demonstrated that the complementary operators yield significant suppression of the artificial reflections at the computational boundaries. Because the COM operation is independent of the wave number, k_x, COM is effective in suppressing reflections from obliquely traveling and evanescent waves. Furthermore, the frequency domain results show that the excellent performance of COM extends across a wide band of frequencies thus facilitating simulation of signals with a very wide dynamic range.

The application of COM calls for two runs of the FDTD code. This initially appears as introducing a significant cost to the simulation. However, it is to be noted that when using COM, the outer boundary can be brought very close to the source of radiation, as was shown in the examples presented, which consequently gives a smaller computational domain requiring fewer time steps to simulate. The smaller computational domain is also advantageous because it keeps numerical dispersion errors to a minimum.

ACKNOWLEDGMENT

The author is grateful to one of the reviewers for indicating the equivalence between $\lim_{A\to\infty}(B_N^*)$ and $\partial_t B_{N-1}$ and for other comments that enhanced the quality of the paper.

REFERENCES

1. A. Bayliss, M. Gunzburger, and T. Turkel, Boundary conditions for the numerical solution of elliptic equations in exterior regions, *SIAM J. Appl. Math.* **42,** 430 (1990).
2. B. Engquist and A. Majda, Radiation boundary conditions for the numerical simulation of waves, *Math. Comput.* **31,** 629 (1977).
3. R. Mittra and O. M. Ramahi, Absorbing boundary conditions for the direct solution of partial differential equations arising in electromagnetic scattering problems, in *Finite Element and Finite Difference Methods in Electromagnetic Scattering* (M. Morgan, Ed., Vol. II, p. 133, (Elsevier Science, New York, 1989).
4. G. Mur, Absorbing boundary conditions for the finite-difference

approximation of the time-domain electromagnetic-field equations, *IEEE Trans. Electromag. Comp.* **EMC23**(4), 377 (1981).

5. R. L. Higdon, Absorbing boundary conditions for difference approximations to the multi-dimensional wave equation, *Math. Comput.* **47**(176), 437 (1986).
6. R. L. Higdon, Radiation boundary conditions for elastic wave propagation, *SIAM J. Numer. Anal.* **27**(4), 831 (1990).
7. Z. P. Liao, H. L. Wong, B. P. Yang, and Y. F. Yuan, A transmitting boundary for transient wave analyses, *Sci. Sinica* (Ser. A **27**(10), 1063 (1984).
8. E. L. Lindman, "Free-space" boundary conditions for the time dependent wave equation, *J. Comput. Phys.* **18,** 66 (1975).
9. B. H. McDonald and A. Wexler, Finite-element solution of unbounded field problems, *IEEE Trans. Microwave Technol.* **MTT-20**(12), 841 (1972).
10. J. De Moerloose and D. De Zutter, Surface integral representation radiation boundary condition for the FDTD method, *IEEE Trans. Antennas Propag.* **41**(7), 890 (1993).
11. O. M. Ramahi, A. Khebir, and R. Mittra, Numerically-derived absorbing boundary conditions for the solution of open region scattering problems, *IEEE Trans. Antennas Propag.* **39**(3), 350 (1991).
12. K. K. Mei, R. Pous, Z. Chen, Y.-W. Liu, and M. D. Prouty, Measured equation of in variance: A new concept in field computations, *IEEE Trans. Antennas Propag.* **42**(3), 320 (1994).
13. B. Stupfel and R. Mittra, Efficiency of numerial absorbing boundary conditions for finite element applications, in *1994 URSI Radio Science Meeting, Symp. Dig., Seattle, Washington, June 19–24, 1994,* 165.
14. J.-P. Berenger, A perfectly matched layer for the absorption of electromagnetic waves, *J. Comput. Phys.,* **114,** 185 (1994).
15. C. M. Rappaport, "Perfectly Matched Absorbing Boundary Conditions Based on Anisotropic Lossy Mapping of Space," *IEEE Microwave and Guided Wave Lett.,* **5**(3), 90 (1995).
16. W. C. Chew and W. H. Weedon, "A 3D perfectly matched medium from modified Maxwell's equations with stretched coordinates," *Microwave and Optical Tech. Lett.,* **7**(13), 599, July 1994.
17. J. De Moerloose and M. Stuchly, "Behavior of Berenger's ABC for evanescent waves," *IEEE Microwave and Guided Wave Lett.,* **5**(10), 344 (1995).
18. B. Chen, D. Fang, and B. H. Zhou, "Modified Berenger PML absorbing boundary condition for FD-TD meshes," *IEEE Microwave and Guided Wave Lett.,* **5**(11), 399 (1995).
19. U. Pekel and R. Mittra, "A finite-element-method frequency-domain application of the perfectly matched layer (PML) concept," *Microwave and Opt. Tech. Lett.,* **9**(3), 117 (1995).
20. O. M. Ramahi, "Application of the complementary operator method to the finite-difference-time-domain solution of the three-dimensional radiation problem," *Microwave and Opt. Tech. Lett.,* **9**(3), 147 (1995).
21. W. D. Smith, "Nonreflecting plane boundary for wave propagation problems," *J. Comput. Phys.,* **15,** 492 (1974).
22. R. L. Higdon, "Absorbing boundary conditions for acoustic and elastic waves in stratified media," *J. Comput. Phys.,* **101,** 386 (1992).
23. R. L. Higdon, Radiation boundary conditions for dispersive waves, *SIAM J. Numer. Anal.* **31**(1), 64 (1994).
24. O. M. Ramahi, "On the use of absorbing boundary conditions in finite difference time domain solutions of unbounded geometry problems," IEEE AP-S/URSI Int. Symp. Dig. Seattle, WA, 168 (1994).
25. K. Demarest, R. Plumb, and Z. Huang, "The performance of FDTD absorbing boundary conditions for buried scatterers," IEEE AP-S/URSI Int. Symp. Dig. Seattle, WA, 169 (1994).
26. W. C. Chew and R. L. Wagner, "A modified form of Liao's absorbing boundary condition," IEEE AP-S/URSI Int. Symp. Dig., Chicago, IL, 536 (1992).
27. M. Moghaddam and W. C. Chew, "Stabilizing Liao's absorbing boundary conditions using single-precision arithmetic," IEEE AP-S/URSI Int. Symp. Dig., London, Ontario, Canada, 430 (1991).
28. A. Taflove, *Computational Electrodynamics: The Finite-Difference Time-Domain Method* (Artech, Boston, 1995).
29. W. C. Chew and J. M. Jin, "Analysis of perfectly-matched layers using lattice EM theory in a discretized world," IEEE AP-S/URSI Int. Symp. Dig. Newport Beach, CA, 338 (1995).
30. A. H. Kamel, "On the accuracy of absorbing boundary conditions for wave propagation," *J. Electromagnetic Wave Appl.,* **8** (5), 647 (1994).